COVID-19 & differential effects in twins: Insights from Placenta Pathology

Kristen Moriarty [a,*], Mingfu Yu [b], Naveed Hussain [c], Kinga Zgutka [c], M. Melinda Sanders [b], Malini Harigopal [d], Jianhui Wang [d], Xi Wang [d], Pei Hui [d], Chen Liu [d], David Sink [c], Andrea Shields [a]

[a] Department of Obstetrics & Gynecology, University of Connecticut, USA
[b] Department of Pathology, University of Connecticut, USA
[c] Department of Pediatrics, Connecticut Children's Medical Center, USA
[d] Department of Pathology, Yale University, USA

A B S T R A C T

Introduction: COVID-19 has been associated with several adverse pregnancy outcomes, including perinatal loss. Differential effects of COVID-19 in a twin pregnancy may provide unique insights into virus-placental interactions. We present a case of perinatal loss of a female fetus with survival of the male co-twin in a pregnancy complicated by COVID-19 and premature delivery.
Methods: Viral detection methods recommended by the NICHD task force were used to identify SARS-CoV-2 and its viral receptors in the placentas and fetal tissue (Antoun et al., 2020) [1]
Results: Compared with the surviving twin, we found a more severe intervillous necrosis and a relatively low detection of ACE2 membranous expression in the syncytiotrophoblasts of the female twin that succumbed.
Discussion: The interactions of SARS-CoV-2 and ACE2 at the maternal fetal interface within the placenta may play a significant role in perinatal loss, and the effects of fetal sex and gestational age at time of infection need to be explored further.

1. Introduction

COVID-19 has been linked to several adverse pregnancy outcomes (APOs) including preterm delivery, low birth weight, fetal growth restriction, stillbirth, and preeclampsia-like syndrome [1–7]. These APOs result in higher NICU admissions, co-morbidities of asphyxia-related complications, hyperbilirubinemia and increased neonatal mortality. The pathogenesis linking COVID-19 and APOs is not entirely clear, but viral-placental interactions have been implicated [8]. SARS-COV-2 is thought to enter the placenta by the spike protein binding to angiotensin-converting enzyme 2 (ACE2). The S protein is then cleaved by transmembrane protease serine 2 (TMPRSS2) allowing cell entry. Levels of ACE2 are theorized to decline throughout pregnancy [9]. Placental changes described in pregnancies complicated by COVID-19 are chronic histiocytic intervillositis, trophoblast necrosis and variable degrees of increased fibrin consistent with massive perivillous fibrin deposition [10–12]. Despite these pathological findings, there is no clear consensus regarding the effect of COVID-19 on stillbirth, and reports of vertical transmission of SARS-CoV-2 remain limited [13,14].

2. Case

A 22-year-old G2P0010 female with dichorionic, diamniotic twin gestation at 27 weeks 0 days presented in preterm labor with intact membranes and COVID-19 infection. Her past medical history was significant for class III obesity, and she was unvaccinated against SARS-CoV-2. Her laboratory evaluation was only remarkable for an elevation in sedimentation rate, procalcitonin and aspartate aminotransferase (AST) and a chest radiograph demonstrated COVID-19 pneumonia. Fetal growth was normal and concordant on ultrasound. She was started and maintained on magnesium for neuroprotection, nifedipine for tocolysis, and vancomycin for group B streptococcus unknown status while receiving celestone for fetal lung maturity. An Infectious Disease consultation was placed with no additional recommendations. Unfortunately, she presented prior to the FDA authorization of monoclonal antibodies to treat mild to moderate COVID-19 patients. Her cervical exam remained unchanged at 48 h and medical interventions were discontinued. Within 4 h of discontinuing medical interventions, a cesarean delivery under general anesthesia was performed due to rapid progression in preterm labor, fetal malpresentation and systemic anticoagulation. The neonatal intensive care unit (NICU) team was present

* Corresponding author. Department of Obstetrics and Gynecology 263 Farmington Ave, Farmington, CT, 06030, USA.
E-mail address: kmoriarty@uchc.edu (K. Moriarty).

for delivery. Twin A, a female, received positive pressure ventilation (PPV), followed by intubation, chest compressions, endotracheal and intravascular epinephrine doses, and normal saline boluses due to an absent heart rate. Heart rate remained undetectable, and resuscitation was stopped at 23 min of life. She had no signs of tissue maceration. At birth, twin B, a male, had poor respiratory effort, and received PPV followed by intubation. After 24 h of life, he was extubated and placed on non-invasive PPV but required re-intubation 12 h later. His SARS-CoV-2 PCR testing at 24 and 48 h of life was negative. His neonatal course was significant for ampicillin-resistant E-coli sepsis at 10 days of life and acquired cytomegalovirus infection at one month. He was discharged home with moderate bronchopulmonary dysplasia and stage 1 retinopathy of prematurity.

The maternal postpartum course was uncomplicated. She recovered from her COVID-19 infection and was discharged on the second postoperative day. She was diagnosed with postpartum adjustment disorder and referred for mental health counseling. Patient consent was obtained for the presentation of this case.

3. Methods

Single nucleotide polymorphism microarray chromosome analysis (ANORA© by Natera™) was performed on twin A. Twin placentas were fixed in formalin and grossly examined with standard sections. Formalin-fixed paraffin-embedded (FPPE) blocks and routine Hematoxylin and Eosin-stained slides were examined. A complete autopsy was performed on twin A using standard protocol.

Immunohistochemistry (IHC) was performed using the anti-SARS-CoV-2 nucleocapsid protein antibody (Thermofisher, mouse monoclonal antibody clone B46D, dilution 1:200). RNA in situ hybridization (ISH) was done using an Advanced Cell Diagnostics anti-SARS-CoV-2 spike protein probe (V-nCoV2019-S, prediluted) using the Leica Bond-III platform (Leica, Wetziar, Germany). All tests were run along with appropriate positive and negative controls. An RNA ISH negative control probe targeting the DapB gene showed appropriate absent background staining. In addition, a positive control probe to the housekeeping gene peptidylpropril isomerase B (PPIB) to assess RNA integrity was included with each run.

A real-time polymerase chain reaction (PCR) test of SARS-CoV-2 was performed using twin placental tissue and fetal tissue from twin A. Briefly, total RNA in FFPE slices was extracted with Promega ReliaPrep FFPE Total RNA Miniprep System. Fifty nanograms of total RNA were imputed as a template for the ThermoFisher TaqPath COVID-19 Real-Time PCR test on 7500 Fast Dx Real-time PCR machine. PCR results were analyzed with 7500 Fast SDS software v1.4.1 and Interpretive Software v1.5. The average Cycle threshold (Ct) values of COVID-19 N gene, S gene, and ORF1ab probes were calculated for each sample. The positive RNA samples were sequenced with Illumina COVIDSeq Test on Illumina NextSeq 550 sequencer, and the consensus genomes were exported through Illumina BaseSpace DRAGEN COVID Lineage pipeline. The genomes were submitted to GISAID database and were input into NextClade and UCSC UShER for phylogeny analysis. Real-time PCR test and genome sequencing of SARS-CoV-2 were processed by the Clinical Molecular Diagnostics Laboratory (Department of Pathology, Yale School of Medicine, 310 Cedar St., New Haven, CT 06510), which is certified under the Clinical Laboratory Improvement Amendments of 1988 (CLIA), 42 USC §263a and meets the requirements to perform high complexity tests.

IHC was performed using the anti-ACE2 antibody (Abcam, rabbit polyclonal antibody, dilution 1:1500). Appropriate positive and negative controls were used.

4. Results

Twin A had a 46, XX karyotype and normal postmortem exam. The Placentae of Twin A and Twin B weighed 161 g and 201 g, respectively.

The dividing membranes were inserted on twin A's placenta and showed dichorionic, diamniotic morphology. The umbilical cords and fetal membranes were unremarkable. Cross-sections of both placentas showed abnormal tan, firm, irregular tissue involving most parenchyma and only a small amount of normal dark, red, and spongy parenchyma. Twin A and twin B placentas grossly appeared similar and differed mildly in the extent of abnormal parenchyma. The abnormal tissue was estimated to involve 95% of placenta volume in twin A and 80–90% in twin B (Fig. 1). Microscopic examination of the placental sections showed marked villous agglutination, and intervillous spaces were mostly obliterated by fibrin, inflammatory cells, and necrotic debris. The chorionic villi exhibited extensive trophoblastic necrosis as illustrated by eosinophilic acellular material, pale stained nuclei, and nuclear debris surrounding the outer layer (Figures 2A to B). The inflammatory cells consisted of abundant histiocytes (highlighted by immunoreactivity to antibodies to CD68 KPM1, Fig. 2C), neutrophils, and scant lymphocytes. There was no apparent vasculopathy on either fetal or maternal vessels.

IHC studies were positive for SARS-CoV-2 in the placental parenchyma for both twin placentas, and the immunoreactivity was concentrated within syncytiotrophoblasts without extending into villous Hofbauer cells or capillaries (Fig. 2D). This positive finding was substantiated by using RNA ISH (Fig. 2E). No immunoreactivity was seen in either fetal, maternal endothelial cells, or decidual cells. Immunostains were negative in the fetal lung and heart (data not shown). There were no convincing cytotrophoblasts appreciated in chorionic villi (relatively normal villi or affected villi) on routine H&E stains or using IHC stains with p63 (data not shown).

ACE2 receptors were localized in syncytiotrophoblasts in viable or less affected chorionic villi; however, no convincing ACE2 staining was appreciated in necrotic trophoblasts (Fig. 2F). ACE2 immunoreactivity was seen in decidual cells but not in maternal or fetal endothelial cells, villous stromal cells, or Hofbauer cells (data not shown). The histologic features, immunostain, RNA ISH results, and ACE2 results were similar in both placentas. Data shown in Fig. 2 are from the placenta of twin A.

PCR results of all tissues tested were positive for SARS-CoV-2, which included 2 FFPE blocks from twin placentas, and the fetal lung and heart of twin A. Cycle threshold (Ct) was negatively associated with the viral load (Fig. 3a to d). The Ct values were low in 2 placental samples, corresponding to a high viral load. Conversely, fetal tissue samples showed high Ct values, therefore, low viral load. Consensus genomes were recovered from two strongly positive samples (placentas) through the Illumina COVIDseq test, while the two weakly positive samples (fetal tissue) failed to give any genome results. In the NextClade database, both genomes were clustered into the 21J (Delta) branch. UCSC UShER confirmed that the two placenta genomes were identical, and both had the R214H mutation in Spike protein and clustered the genomes into lineage AY.44, a subgroup of delta, which was consistent with the MassARRAY result reported by the State of Connecticut DPH lab from the mother's nasopharyngeal swab. The placenta viral genomes are published on GISARD. The GISAID IDs are EPI_ISL_7803591 for placenta A and EPI_ISL_7803592 for placenta B.

5. Discussion

The novel contribution of this case report is the identification of SARS-CoV-2 in the placental and fetal tissue in a mother-twin triad, confirming placenta infection using standardized definitions proposed by the Eunice Kennedy Shriver National Institute of Child Health and Human Development (NICHD) SARS-CoV-2 Placental Infection Workshop. Furthermore, we demonstrated vertical/transplacental transmission of SARS-CoV-2 and the correlation between the viral receptor concentration in each placenta and differential outcomes between the demised and surviving twin [7,15]. Normal trophoblasts function as a barrier preventing pathogens passing from mothers to fetuses. SARS-CoV-2 viral particles reach the placentas through viremia and then
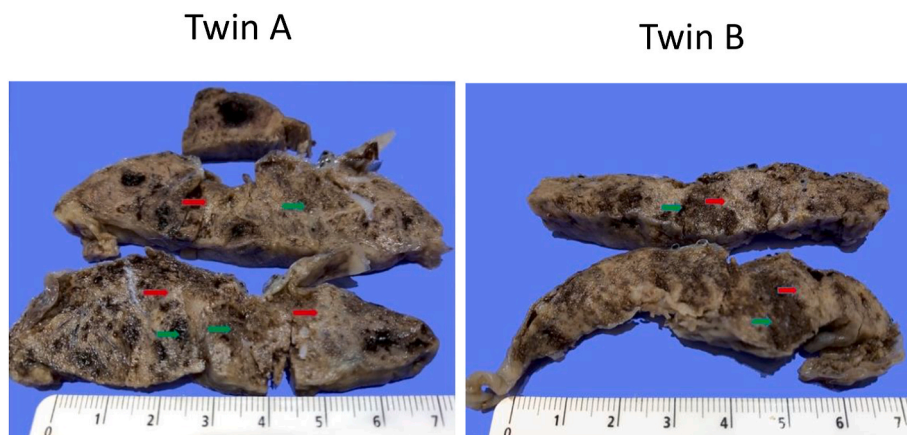
Twin A

Twin B

Fig. 1. Cross sections of placenta parenchyma. Both placentas show tan, firm abnormal tissue (red arrows); only scant normal appearing dark red and spongy parenchyma is seen (green arrows).
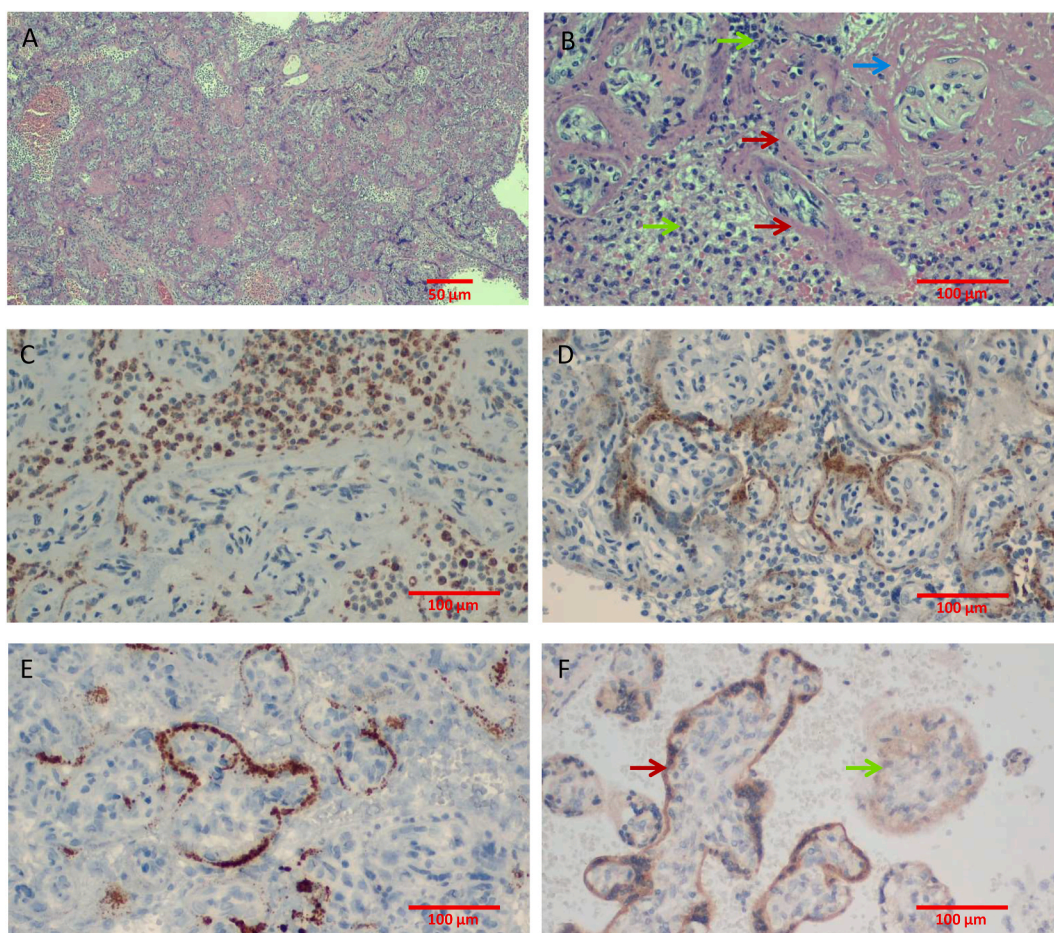

Fig. 2. Placenta from twin A. A: low power shows agglutinated villi with obliterated Intervillous spaces (4x). B: Higher power shows trophoblastic necrosis (red arrows), Inflammatory cell infiltrates in intervillous spaces (green arrows), and fibrin (blue arrows). C: Immunohistochemistry with CD68 demonstrates histiocytic intervillositis (brown stain). D: Immunohistochemistry with antibody to COVID-19 nucleocapsid protein shows strong Immunoreactivity in syncytialtrophoblasts (brown stain). E: RNA ISH using probes for COVID-19 spike protein exhibits strong signals in syncytialtrophoblasts (brown granular Stains). F: Immunostain for ACE2 receptors illustrates positive staining within viable Syncytiotrophoblast (red arrows), while non-viable villi without apparent signal (green Arrow, background stain). B to F: 20x

interact with ACE2 receptors, normally located within syncytial trophoblasts [16]. The viruses eventually cause trophoblastic necrosis and weaken the maternal/fetal barrier. Our PCR data shows a significant viral load reduction from the placenta to fetal tissue. The viral proteins (nucleocapsid or spike proteins) were not identified by IHC and RNA ISH in fetal tissue and were only detected by highly sensitive methodology, such as PCR. The low viral load in fetal tissue likely does not cause discernible changes in the fetus, as evident from a normal fetal autopsy. It is likely that fetal demise is caused predominantly, if not solely, by placental malfunction.
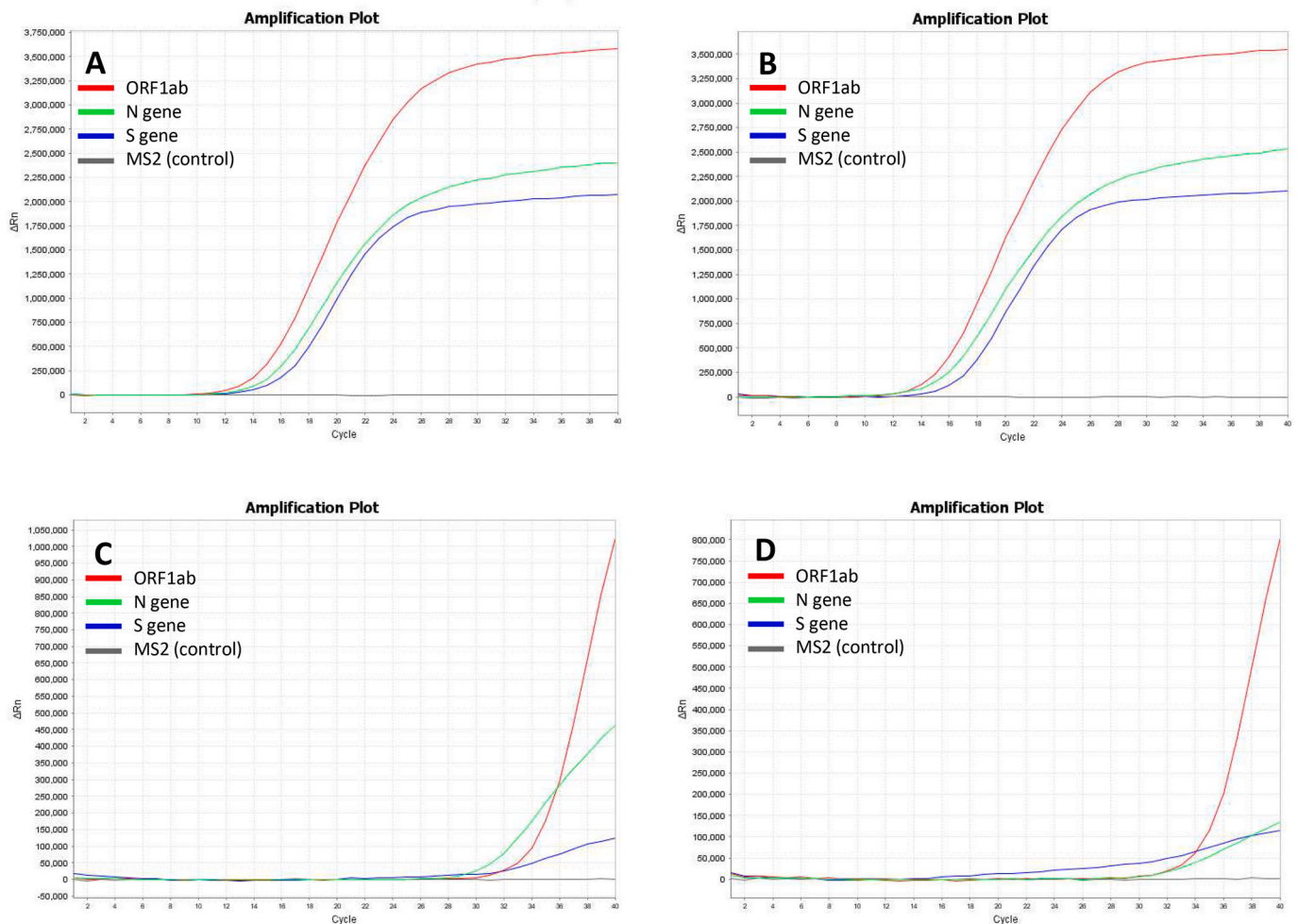
Fig. 3. Real time PCR of 4 patient samples are all positive for COVID-19 signals (ORF1ab, N gene, and S gene).Control signal MS2 is not amplified.A: Twin A placenta. Cycle threshold (Ct) 14 B: Twin B placenta. Ct 14 C: Fetal lung. Ct 33 D: Fetal heart. Ct 34.

The relationship between SARS-CoV-2 invasion of the placenta at the maternal-fetal interface may depend on the available receptors, ACE2 or Transmembrane Serine Protease 2 (TMPRSS2) [6,17]. In reviewing the presence of ACE2 in all human tissues, Hikmet et al. noted ACE2 expression in placental trophoblasts [18]. Within the placental tissue, ACE2 membranous expression was demonstrated in the syncytio-trophoblast (ST) of chorionic villi predominantly in a polarized pattern, with expression highest on the maternal side of the syncytiotrophoblast. In addition, Schwartz et al. found that cytotrophoblast and extra-villous trophoblasts express ACE2, but no ACE2 expression was detected in villous stroma, Hofbauer cells, or endothelial cells [10]. During fetal development, the co-expression of ACE2 and TMPRSS2 genes is seen in the trophoblast of the blastocyst, syncytiotrophoblast, and hypoblast of the implantation stages after seven weeks of conception, which relates to the maternal blood supply for the fetus [8]. Interestingly, in several studies, placental findings demonstrated that syncytiotrophoblasts are often infected with SARS-CoV-2, but fetuses are not always infected [2, 16]. These findings suggest the presence of a placental barrier, even if it is not entirely adequate. The association of second trimester ACE2+ TMPRSS2+ trophoblasts with Toll-like receptor pathway may offer in-sights into the potential barrier effects of these with respect to SARS-CoV-2 attacking the maternal-fetal interface [19]. It is possible that the expression of ACE2 in the placental trophoblasts, which is highest in early gestation, wanes with increasing gestational age and is relatively low close to term gestation [6]. There are other proteins in the placenta that interact with SARS-CoV-2, which may also modulate the effect of the virus [12].

Standardized methods for diagnosing placental infection by SARS-CoV-2 have recently been proposed by the Eunice K. Shriver NICHD SARS-CoV-2 Placental Workshop to provide guidelines for research and clinical care [7]. Five levels of rigor for detecting placental infection with SARS-CoV-2 and corresponding diagnostic criteria were defined. Our approach to pathological examination of the twin placentas and fetal autopsy will facilitate future investigations into this area using these rigorous criteria.

Our case of dichorionic diamniotic twins offers a novel insight into the pathogenesis of COVID-19-related fetal morbidity and mortality. The differential effect of the virus on the two placentas may have been responsible for the alternate outcome of the newborn twins. The twin that succumbed showed a more severe intervillous necrosis associated with a relatively low detection of the ACE2 in the affected regions. The surviving twin had relatively more areas of ACE2 staining that persisted and a relatively lower extent of intervillositis. It is unclear if the dif-ference in ACE2 expression was related to necrosis or other factors such as sex differences. It is possible that a critical threshold for placental dysfunction from infection-induced necrosis, genetic heterogeneity of the ACE2 receptor, fetal sex-related differences in ACE2, or other heretofore unknown factors may have contributed to the differential results in these twins. The interactions of SARS-CoV-2 and ACE2 at the maternal fetal interface within the placenta and its impact on pregnancy outcomes needs further investigation.

Declaration of competing interest

None.

References

[1] L. Antoun, N.E. Taweel, I. Ahmed, S. Patni, H. Honest, Maternal COVID-19 infection, clinical characteristics, pregnancy, and neonatal outcome: a prospective cohort study, Eur. J. Obstet. Gynecol. Reprod. Biol. 252 (2020) 559–562.

[2] A. Lu-Culligan, A.R. Chavan, P. Vijayakumar, L. Irshaid, E.M. Courchaine, K. M. Milano, et al., Maternal respiratory SARS-CoV-2 infection in pregnancy is associated with a robust inflammatory response at the maternal-fetal interface, Med (N Y). 2 (5) (2021) 591–610 e10.

[3] M. Mendoza, I. Garcia-Ruiz, N. Maiz, C. Rodo, P. Garcia-Manau, B. Serrano, et al., Pre-eclampsia-like syndrome induced by severe COVID-19: a prospective observational study, BJOG 127 (11) (2020) 1374–1380.

[4] B.R. Mercedes, A. Serwat, L. Naffaa, N. Ramirez, F. Khalid, S.B. Steward, et al., New-onset myocardial injury in pregnant patients with coronavirus disease 2019: a case series of 15 patients, Am. J. Obstet. Gynecol. 224 (4) (2021) 387 e1–e9.

[5] S. Wang, L. Guo, L. Chen, W. Liu, Y. Cao, J. Zhang, et al., A case report of neonatal 2019 coronavirus disease in China, Clin. Infect. Dis. 71 (15) (2020) 853–857.

[6] J. Zhou, S. Choi, H. Liu, J. Zhang, Y. Tian, A.G. Edlow, et al., Is SARS-CoV-2 infection a risk factor for early pregnancy loss? ACE2 and TMPRSS2 coexpression and persistent replicative infection in primitive trophoblast, J. Infect. Dis. 224 (Suppl 6) (2021) S660–S669.

[7] D.J. Roberts, A.G. Edlow, R.J. Romero, C.B. Coyne, D.T. Ting, J.L. Hornick, et al., A standardized definition of placental infection by SARS-CoV-2, a consensus statement from the national institutes of health/eunice Kennedy shriver national Institute of Child health and human development SARS-CoV-2 placental infection Workshop, Am. J. Obstet. Gynecol. 225 (6) (2021) 593 e1–e9.

[8] B.A.T. Weatherbee, D.M. Glover, M. Zernicka-Goetz, Expression of SARS-CoV-2 receptor ACE2 and the protease TMPRSS2 suggests susceptibility of the human embryo in the first trimester, Open Biol 10 (8) (2020) 200162.

[9] D.A. Schwartz, E. Avvad-Portari, P. Babal, M. Baldewijns, M. Blomberg, A. Bouachba, et al., Placental tissue destruction and insufficiency from COVID-19 causes stillbirth and neonatal death from hypoxic-ischemic injury: a study of 68 cases with SARS-CoV-2 placentitis from 12 countries, Arch. Pathol. Lab Med. (2022) 1–26. Submitted for publication, https://meridian.allenpress.com/aplm/article/doi/10.5858/arpa.2022-0029-SA/477699/Placental-Tissue-Destruction-and-Insufficiency.

[10] D. Morotti, M. Cadamuro, E. Rigoli, A. Sonzogni, A. Gianatti, C. Parolin, et al., Molecular Pathology analysis of SARS-CoV-2 in syncytiotrophoblast and hofbauer cells in placenta from a pregnant woman and fetus with COVID-19, Pathogens 10 (4) (2021).

[11] D.A. Schwartz, D. Morotti, Placental Pathology of COVID-19 with and without fetal and neonatal infection: trophoblast necrosis and chronic histiocytic intervillositis as risk factors for transplacental transmission of SARS-CoV-2, Viruses 12 (11) (2020).

[12] A.A. Seethy, S. Singh, I. Mukherjee, K. Pethusamy, K. Purkayastha, J.B. Sharma, et al., Potential SARS-CoV-2 interactions with proteins involved in trophoblast functions - an in-silico study, Placenta 103 (2021) 141–151.

[13] E.V. Kingston, High rates of stillbirth and preterm delivery in women with covid-19 and the efficacy of ECMO in pregnancy, BMJ 370 (2020) m2921.

[14] B. Pasternak, M. Neovius, J. Soderling, M. Ahlberg, M. Norman, J.F. Ludvigsson, et al., Preterm birth and stillbirth during the COVID-19 pandemic in Sweden: a nationwide cohort study, Ann. Intern. Med. 174 (6) (2021) 873–875.

[15] T. Mok, D. Contreras, R.H. Chmait, J. Goldstein, I.D. Pluym, K. Tabsh, et al., Complicated monochorionic-diamniotic twins in a pregnant woman with COVID-19 in the second trimester, Am. J. Perinatol. 38 (7) (2021) 747–752.

[16] S. Komine-Aizawa, K. Takada, S. Hayakawa, Placental barrier against COVID-19, Placenta 99 (2020) 45–49.

[17] E. Taglauer, Y. Benarroch, K. Rop, E. Barnett, V. Sabharwal, C. Yarrington, et al., Consistent localization of SARS-CoV-2 spike glycoprotein and ACE2 over TMPRSS2 predominance in placental villi of 15 COVID-19 positive maternal-fetal dyads, Placenta 100 (2020) 69–74.

[18] F. Hikmet, L. Mear, A. Edvinsson, P. Micke, M. Uhlen, C. Lindskog, The protein expression profile of ACE2 in human tissues, Mol. Syst. Biol. 16 (7) (2020), e9610.

[19] N. Ashary, A. Bhide, P. Chakraborty, S. Colaco, A. Mishra, K. Chhabria, et al., Single-cell RNA-seq identifies cell subsets in human placenta that highly expresses factors driving pathogenesis of SARS-CoV-2, Front. Cell Dev. Biol. 8 (2020) 783.